A sensation for inflation: initial swim bladder inflation in larval zebrafish is mediated by the mechanosensory lateral line.

Alexandra Venuto[1], Stacey Thibodeau-Beganny[2], Josef G. Trapani[2], Timothy Erickson[3]

1. Department of Biology, East Carolina University, Greenville, NC, USA.
2. Department of Biology and Neuroscience Program, Amherst College, Amherst, MA, USA.
3. Department of Biology, University of New Brunswick, Fredericton, NB, Canada.

Abstract

Larval zebrafish achieve neutral buoyancy by swimming up to the surface and taking in air through their mouths to inflate their swim bladders. We define this behavior as 'surfacing'. Little is known about the sensory basis for this underappreciated behavior of larval fish. A strong candidate is the mechanosensory lateral line, a hair cell-based sensory system that detects hydrodynamic information from sources like water currents, predators, prey, and surface waves. However, a role for the lateral line in mediating initial inflation of the swim bladder has not been reported.

To explore the connection between the lateral line and surfacing, we utilized a genetic mutant (*lhfpl5b*$^{-/-}$) that renders the zebrafish lateral line insensitive to mechanical stimuli. We observe that approximately half of these lateral line mutants over-inflate their swim bladders during initial inflation and become positively buoyant. Thus, we hypothesize that larval zebrafish use their lateral line to moderate interactions with the air-water interface during surfacing to regulate swim bladder inflation. To test the hypothesis that lateral line defects are responsible for swim bladder over-inflation, we show exogenous air is required for the hyperinflation phenotype and transgenic rescue of hair cell function restores normal inflation. We also find that chemical ablation of anterior lateral line hair cells in wild type larvae causes hyperinflation. Furthermore, we show that manipulation of lateral line sensory information results in abnormal inflation. Finally, we report spatial and temporal differences in the surfacing behavior between wild type and lateral line mutant larvae. In summary, we propose a novel sensory basis for achieving neutral buoyancy where larval zebrafish use their lateral line to sense the air-water interface and regulate initial swim bladder inflation.

Keywords: behavior, buoyancy, hair cells, hydrodynamics, lateral line, lhfpl5, swim bladder, sensory system, zebrafish

Introduction

The swim bladder of teleost fish provides for neutral buoyancy in the water column, thereby minimizing the energy expenditure associated with locomotion [1]. Larval teleosts initate swim bladder inflation by swimming up to the surface to ingest air using a set of behaviors we refer to as "surfacing" [2–4]. Although surfacing poses a significant risk of predation, larval fish are highly motivated to reach the surface to intake air. For example, pre-inflated lake trout larvae will swim hundreds of feet at a constant rate in attempts to access the surface [5]. Surfacing is a complex task that requires a combination of newly developed physical features, sensory systems, and motor skills [6–10] – (i) Larvae must discriminate up from down and (ii) be able to move directionally towards the surface; (iii) they must appropriately sense the air-water interface, and (iv) be able to intake air through the mouth upon arrival at the surface. Ingested air is then moved by peristalsis into the swim bladder through the pneumatic duct that connects the gut and swim bladder [5,10,11]. Together, surfacing represents perhaps the most complex behavior that larvae perform prior to achieving neutral buoyancy [12].

Little is known about the sensory cues that instruct the surfacing behavior. Perturbations to the vestibular system typically result in hypoinflation [13,14]. The inability to detect gravity by the utricular otolith is specifically responsible for the phenotype, presumably because larvae are unable to orient their movements upwards towards the surface [15]. Photosensory cues may also play a role in directional orientation and surface detection. However, which photosensory systems are involved has not been defined and the effects of altering lighting conditions varies between species [16–18]. Even less is known about how larval fish detect the air-water interface itself. Fish and some amphibians possess an additional hair cell-based sensory system - the *mechanosensory lateral line* - that contributes to detection of near-field hydrodynamic information originating from water currents, predators and prey, conspecifics, abiotic objects, and surface waves [19–26]. Specific to surface detection, surface-feeding fish use their lateral line to detect surface waves created by their prey [27]. Furthermore, Japanese flying fish are predicted to use their ventrally-located lateral line to sense transitions through the air-water interface [28,29]. While the lateral line is a strong candidate to aid in surfacing behaviors that lead to initial swim bladder inflation in larval fish, its specific role in this important behavior has not been explored.

A CRISPR-Cas9 knockout of *LHFPL tetraspan subfamily member 5b* (*lhfpl5b*) is the first genetic zebrafish mutant where the lateral line is non-functional from birth but hearing and balance

are normal [30]. These mutants provide an opportunity to uncover novel roles for the lateral line. Unexpectedly, homozygous mutant larvae present with a hyperinflation phenotype characterized by over-filled swim bladders and positive buoyancy, a very rare finding among swim bladder defects [31,32]. Using several genetic and chemical techniques to manipulate lateral line function, we show that lateral line sensory information is used by larval zebrafish to appropriately fill their swim bladders, likely by detecting surface tension at the air-water interface using mechanosensory neuromasts located on their heads. Overall, our study uncovers a novel role for the mechanosensory lateral line mediating initial inflation of the swim bladder.

Methods

Animal husbandry and ethics statement

Adult zebrafish (*Danio rerio*) were maintained and bred using standard procedures [33]. All experiments used larvae at 2-6 days post-fertilization (dpf), which are of indeterminate sex at this stage. Except where otherwise stated, animals were placed in clear, plastic tubs (dimensions: 15 cm x 10 cm x 4 cm, E3 volume: 460 mL) at 2 dpf and maintained at 28.5°C on a 14:10 light/dark cycle at 500-700 lux in E3 embryo media (5 mM NaCl, 0.17 mM KCl, 0.33 mM CaCl2, 0.33 mM MgCl2, buffered with NaHCO3). Animal research complied with guidelines stipulated by the Institutional Animal Care and Use Committees at East Carolina University (protocol D372) and Amherst College (assurance number 3925-1 with the Office of Laboratory Animal Welfare).

Mutant and transgenic fish lines

The zebrafish mutant allele *lhfpl5b*^{vo35} and transgenic lines *Tg(myo6b:EGFP-lhfpl5a)vo23* and *Tg(myo6b:EGFP-PA)vo68* were used in this study [30,34]. For all experiments, *lhfpl5b*^{vo35} homozygotes were identified from their hetero- and homozygous wild type siblings by lack of FM 1-43 (ThermoFisher) labeling of the lateral line hair cells.

To create a fish line that expresses the Channelrhodopsin-2 (ChR2) optogenetic protein solely in the hair cells of the lateral line, approximately 2 kb of DNA upstream of the start codon of the *lhfpl5b* gene was cloned into the p5E plasmid of the recombination-based multisite Gateway cloning system (ThermoFisher). A Tol2 transposon backbone was then used to create the injectable expression plasmid *lhfpl5b2028:ChR2-EYFP-PA*. This plasmid was then co-injected with transposase mRNA into single-cell embryos [35] to create the *Tg(lhfpl5b2028:ChR2-EYFP-PA)* zebrafish line.

Buoyancy tests

To ascertain the buoyancy status of larval fish, larvae were anesthetized with MS-222 (Western Chemical Inc., Ferndale, WA) and placed at the vertical midway point of a 50 mL conical tube containing E3 media. At the expiration of a 30-second timer, the end position of the fish was recorded and the fish was removed from the tube for imaging under the microscope. If the fish reached the top or bottom of the tube before 30 seconds, then the time it took to reach that location was recorded. The total height of the water column was 8.9 cm, and the fish was placed half-way at 4.45 cm. The rate of buoyancy was determined by dividing the centimeters travelled by the seconds it took to travel that distance (cm/s).

Imaging and swim bladder measurements

Swim bladders were imaged using a SteREO Discovery.V8 microscope (Zeiss) equipped with a Gryphax Arktur camera (Jenoptik). Lateral and dorsal images of the swim bladder were taken for each fish. Swim bladder measurements were conducted using the measurement tool in Adobe Photoshop where measurements were calibrated according to the image of the stage micrometer taken when imaging experiments. The major axis and minor axis of the lateral view of the swim bladder was measured as well as the minor axis of the dorsal view. All measurements were taken from numbered images so that the measurer was blinded to the genotype/condition. These meaurements were halved and used in the equation for the volume of an ellipsoid: $V = 4/3\pi abc$ to find the volume of the swim bladder [2]

Manipulation of photosensory cues during surfacing

At 0 dpf, zebrafish embryos were collected and immediately placed in plastic tubs filled with E3 (detailed above) in an unlit incubator. Larvae were not brought into light until 6 dpf, at which point lateral line mutants and wild type siblings were identified by FM 1-43 labeling. After sorting, larvae were analyzed for buoyancy. The experiment was repeated three times using 20-21 larvae (combined mutant and wild type) per trial.

Blocking access to the air-water interface

Mutant larvae and wild type siblings were sorted at 2 dpf into glass cylinders (diameter: 9.5 cm, E3 volume: 425 mL) equipped with fitted, wire mesh filter plungers (Bodum Inc., USA). Conditions were as follows: wild type with open access to the surface, wild type with blocked access to the surface, mutant with open access to the surface, and mutant with blocked access to

122 the surface. All containers were filled half way with E3 and in the experimental condition ("blocked
123 access"), the filter was pressed down below the surface for both wild type and mutant larvae. The
124 control condition used the same amount of E3 but the filter remained above the surface so that
125 larvae could access the exogenous air. Conditions remained constant until 6 dpf when larvae were
126 imaged and analyzed for swim bladder inflation. The experiment was repeated three times using
127 15-25 larvae per condition.

128 *Analysis of surfacing behavior*

129 Wild type and *lhfpl5b*^{vo35} larvae were blocked from having access to the surface until 9 AM
130 on 4 dpf when individuals were immediately placed into clear rectangular containers (dimensions:
131 3 cm x 3 cm x 3 cm, E3 volume: 20 mL) for video recording. Recordings lasted 12 hours, from 9
132 AM to 9 PM on 4 dpf. At the end of filming, larvae were imaged and analyzed for buoyancy and
133 swim bladder volume, as described. All surfacing videos were numbered for blind analysis.
134 Surfacing analysis was conducted by manual observation of each individual larvae from the videos
135 (30 frames per second) and manually counting visits made to the surface (counted as reaching the
136 meniscus), the timeframe of the video at which the surfacing event occurred, and the duration of
137 time spent at the surface per surfacing event. Recording was repeated six times with 3 mutant and
138 2 wild type larvae per recording. Larvae that did not inflate their swim bladders by the end of
139 filming were excluded from this analysis due to lack of surfacing events.

140 *Lateral line hair cell ablations*

141 For all experiments, wild type and *lhfpl5b* mutant larvae were treated with ototoxin with
142 untreated siblings acting as controls (n = 7-15 larvae per condition per trial, 4 trials) For single
143 treatments, surface accessed was blocked as described above for untreated and treated larvae until
144 9 AM on 4 dpf when treatment occurred. Single 30 minute treatments with neomycin sulfate (EMD
145 Millipore Corp., USA) were done with a 100 µm solution in E3 while repeated neomycin
146 treatments [36] were done as previously described with a concentration of 50 µM. For full ablation
147 with copper sulfate (CuSO4; Ward's Science, Rochester, NY), the treatment concentration was 10
148 uM with a 30 minute exposure. For experiments where head and trunk neuromasts were selectively
149 ablated, we anesthetized the larvae and pipetted them on agarose gel. Excess water was removed
150 and a thin layer of petroleum jelly (Vaseline, Unilever USA) was placed horizontally at the back
151 of the head. Next, 30 uM CuSO4 or E3 was pipetted onto the appropriate region depending on the
152 experimental condition. Immediately follow the 13 minute treatment, larvae were placed in fresh

153 E3 in clear tubs detailed above for 24 hours until 9 AM on 5 dpf when larvae were imaged and
154 analyzed for swim bladder inflation. For all experiments, larvae were imaged and analyzed for
155 swim bladder inflation at 9 AM on 5 dpf. Each experiment was repeated three times using 10-24
156 larvae per condition.

157 *Transgenic rescue of lateral line mutant*

158 Larval zebrafish from crosses of *lhfpl5b*$^{+/-}$ and *Tg(myo6b:EGFP-lhfpl5a)vo23Tg; lhfpl5b*$^{+/-}$
159 were sorted at 2 dpf for transgene expression. At 6 dpf, larvae were numbered, imaged for swim
160 bladder inflation and genotyped for the *lhfpl5b*^{vo35} allele as previously described [30]. The
161 experiment was repeated twice using 26-48 larvae per condition.

162 *Optogenetic activation of lateral line hair cells with Channelrhodopsin-2 (ChR2)*

163 After blocking access to the surface until 4 dpf, we exposed wild type and lateral line
164 mutants, with or without the *lhfpl5b2028:ChR2-EYFP-PA* transgene, to LED blue light (470 nm)
165 with an intensity of 730 lux over their holding tanks against a dark background. Light flashed for
166 25 milliseconds with a one second delay between each pulse. Control larvae were kept in the same
167 background, without blue light exposure. Conditions were held constant until 6 dpf when larvae
168 were imaged and analyzed for swim bladder inflation. The experiment was repeated three times
169 using 15-25 larvae per condition.

170 *Oil-water interface experiments*

171 Mutant larvae and wild type siblings were sorted into clear cylindrical containers (diameter:
172 5 cm , volume: 60 mL) with embryo media only or embryo media with a 2 mm thick surface layer
173 of lab grade mineral oil (Ward's Science, Rochester, NY). Oil on the surface decreases surface
174 tension [37] and has been previously used in experiments involving the zebrafish swim bladder
175 [38]. Conditions remained constant until 6 dpf when larvae were imaged and analyzed for swim
176 bladder volume. Because oil-filled larvae are negatively buoyant, we did not perform buoyancy
177 tests and classified larvae as over-filled based on swim bladder volume alone. The experiment was
178 repeated three times using 15-25 larvae per condition.

179 *Graphs and statistical tests*

180 All graphs and statistical tests were done using R [39]. One-way ANOVAs were used to
181 compare the conditions as a whole (genotype independent variable plus environment independent
182 variable) with Tukey post-hoc test. Chi-squared tests were used to analyze proportion data for over

183 and under-inflation. For the over-inflation comparisons, the two categories used in the comparison
184 between conditions/genotypes were (i) over-inflation and (ii) all other inflation (regular and under),
185 meaning that totals per category/genotype accounted for 100% of the population. Similarly, for the
186 under-inflation comparisons, the two categories used in the comparison between
187 conditions/genotypes were (i) under-inflation and (ii) all other inflation (regular and over). P-values
188 less than 0.05 were considered significant.

189 **Results**

190 *Lateral line mutants exhibit a swim bladder hyperinflation phenotype*

191 The lateral line has not been previously implicated in initial inflation of the larval swim
192 bladder. As such, it was unexpected to observe that lateral line mutants (*lhfpl5b*$^{-/-}$) exhibit
193 hyperinflated swim bladders by 5-6 dpf (Figure 1A). We measured swim bladder volume and
194 buoyancy for each larva in the mutant and wild type populations (Figure 1B) and found that, on
195 average, 53.7% (*SD* = 6.4%, *n* = 41) of lateral line mutants over-inflate their swim bladders and
196 7.3% (SD = 7.1%, *n* = 41) under-inflate. For wild type larvae (including *lhfpl5b*^{vo35} heterozygotes),
197 0.0% (*SD* = 0.0%, *n* = 41) over-inflate and 4.9% (*SD* = 3.7%, *n* = 41) under-inflate their swim
198 bladders during initial inflation on average (Figure 1C). The proportion of over-inflation is
199 significantly different between mutant and wild type larvae (chi-square statistic: 70.45, $p <$
200 0.00001), while the proportion of under-inflation is not (chi-square statistic: 0.3546, $p = 0.552$).
201 Average swim bladder volume of mutant fish is larger ($M = 0.012$ mm^3, $SD = 0.002$ mm^3) than
202 wild type siblings ($M = 0.0058$ mm^3, $SD = 0.00043$ mm^3, $t(80) = 17.4$, $p < 0.0001$) (Figure 1D).
203 The proportions of neutrally and positively buoyant larvae do not change when raised in total
204 darkness (Supplemental Figure 1). This unexpected hyperinflation phenotype in *lhfpl5b*^{vo35}
205 homozygotes led us to investigate if the lateral line is contributing important sensory information
206 during the surfacing behavior.

207 *Access to the air-water interface is required for the hyperinflation phenotype of lateral line mutants*

208 For most teleosts, initial swim bladder inflation requires an intake of exogenous air,
209 typically from the water's surface. To test if the hyperinflation phenotype of lateral line mutants
210 requires access to surface air, we physically blocked access to the surface from 2-6 dpf (Figure 2).
211 On average, 0% (*SD* = 0.0%, *n* = 43) of blocked *lhfpl5b* mutants over-inflate their swim bladders,
212 which is significantly different from mutants with access to the surface (chi-square statistic: 70.45,
213 $p < 0.00001$; Figure 2B). The average swim bladder volume of blocked mutants ($M = 0.0033$ mm^3,

214 *SD* = 0.0015 mm^3) is significantly smaller than mutants with open access (*M* = 0.014 mm^3, *SD* =
215 0.0027 mm^3) (One-way ANOVA with Tukey post-test, $p < 0.00001$). Blocked mutant larvae had
216 statistically similar swim bladder volumes to blocked wild type larvae (*M* = 0.0037 mm^3, *SD* =
217 0.001 mm^3) (One-way ANOVA with Tukey post-test, $p = 0.927$) (Figure 2C). From these data, we
218 conclude that the *lhfpl5b* mutant hyperinflation phenotype requires intake of exogenous air and is
219 not caused by abnormal gas exchange from surrounding media nor excess internal gas production.

220 *Transgenic rescue of lateral line mutants restores normal inflation*

221 We next examined if lateral line defects are responsible for the hyper-inflation phenotype
222 of *lhfpl5b* mutants by restoring lateral line function in mutant larvae. We used the
223 *Tg(myo6b:EGFP-lhfpl5a)vo23* transgene, which uses a hair cell specific promoter (*myo6b*) to drive
224 a GFP-tagged *lhfpl5a* gene [34]. It has been shown that this *lhfpl5a* transgene rescues lateral line
225 hair cell function in *lhfpl5b*$^{-/-}$ *(or* lateral line) mutant fish [30]. Using this rescue method, we
226 observe no cases of hyperinflation in transgenic mutants (0%, *SD* = 0.0%, *n* = 17), which is
227 significantly different from non-transgenic mutants (chi-square statistic: 82.12, $p < 0.00001$; Figure
228 3A). The average volume of the transgenic mutant swim bladder (*M* = 0.0057 mm^3, *SD* = 0.00001
229 mm^3) is significantly smaller than non-transgenic, *lhfpl5b* mutant siblings (*M* = 0.0109 mm^3, *SD* =
230 0.0031 mm^3) (One-way ANOVA with Tukey post-test, $p = 0.000003$), but statistically similar to
231 that of wild type transgenics (*M* = 0.0057 mm^3, *SD* = 0.0005 mm^3) (One-way ANOVA with Tukey
232 post-test, $p = 0.979$, Figure 3B). Because the restoration of *lhfpl5* function specifically in hair cells
233 mitigates hyperinflation in *lhfpl5b* mutants, we conclude that the phenotype is due to defects in
234 sensory hair cell function and not caused by an unrecognized role for *lhfpl5b* in another sensory
235 organ or the swim bladder itself.

236 *Selective ablation of head neuromasts produces a hyperinflation phenotype in wild type larvae*

237 To further test if lateral line defects are responsible for the hyper-inflation phenotype seen
238 in *lhfpl5b* mutants, we ablated lateral line hair cells in wild type larvae using either neomycin
239 sulfate (neo) or copper sulfate (CuSO4) (Supplemental Figure 2 and Figure 4). Administering either
240 single or repeated neomycin treatments during the initial swim bladder inflation period of 3 - 4 dpf
241 results in a significant increase in the proportion of positively buoyant larvae (single neo chi-square
242 statistic: 9.95, $p = 0.0016$, repeated neo chi-square statistic: 34.88, $p < 0.0001$; Supplemental Figure
243 2A), but a non-significant increase in the average swim bladder volume (One-way ANOVA with
244 Tukey post-test, single neo $p = 1.0$, repeated neo p = 0.578; Supplemental Figure 2B). By

245 comparison, a single CuSO4 treatment results in a hyperinflation phenotype that is statistically
246 indistinguishable from lateral line mutants. An average of 59.6% (*SD* = 7.7%, *n* = 72) of CuSO4-
247 treated wild types over inflate their swim bladders, which is significantly different from wild type
248 controls (chi-square statistic: 39.69, $p < 0.0001$; Supplemental Figure 2A). The average swim
249 bladder volume of the CuSO4-treated wild type larvae (*M* = 0.0126 mm^3, *SD* = 0.0027 mm^3) is
250 statistically similar to the average swim bladder volume of untreated lateral line mutants (*M* =
251 0.0139 mm^3, *SD* = 0.0007 mm^3) (One-way ANOVA with Tukey post-test, $p = 0.813$)
252 (Supplemental Figure 2B).

253 Since the anterior lateral line is likely to be the only part of the sensory organ to interact
254 with the air-water interface during surfacing, we predict that disruption of the head neuromasts will
255 result in hyperinflation and that trunk neuromasts will not play a role (Figure 4, Supplemental
256 Figure 3). Selective ablation of the anterior region with CuSO4 results in an average of 35.9% (*SD*
257 = 10.1%, *n* = 38) hyperinflated larvae, which is significantly different from unablated controls (chi-
258 square statistic: 39.69, $p < 0.0001$; Figure 4B). Wild type larvae with head-specific ablations exhibit
259 a significant increase in average swim bladder volume (*M* = 0.016 mm^3, *SD* = 0.0013 mm^3)
260 compared to untreated wild type siblings (*M* = 0.0012 mm^3, *SD* = 0.0013 mm^3) (One-way ANOVA
261 with Tukey post-test, $p = 0.0365$) and statistically comparable swim bladder volumes to that of full
262 CuSO4-treated larvae (*M* = 0.016 mm^3, *SD* = 0.0029 mm^3) (One-way ANOVA with Tukey post-
263 test, $p = 0.987$) (Figure 4C). Conversely, tail-specific CuSO4 treatments do not cause
264 hyperinflation in wild type fish and result in statistically similar swim bladder volumes to untreated
265 siblings (*M* = 0.012 mm^3, *SD* = 0.0031 mm^3) (One-way ANOVA with Tukey post-test, $p = 0.835$)
266 (Figure 4C). The *lhfpl5b* mutant hyperinflation phenotype was not affected by either neomycin or
267 CuSO4 treatments (Supplemental Figure 2). Taken together, we conclude that the anterior region
268 of the lateral line system is critical to surface detection during initial swim bladder inflation.

269 *Decreasing surface tension results in over-filling of the swim bladder*

270 Surface tension is a characteristic that makes the air-water interface distinct from the rest
271 of the water column. We predict that larval fish sense this stimulus with their anterior lateral line
272 neuromasts and that by decreasing the interfacial tension, we would observe abnormal swim
273 bladder inflation in wild type larvae while lateral line mutants would be unaffected. The interfacial
274 tension between oil and water is approximately half that of air and water [37]. We layered oil onto
275 the surface of the embryo media and allowed larvae to perform surfacing behaviors between 2-6

276 dpf (Figure 5). Using this experimental design, we find that the average swim bladder volume of
277 wild types exposed to an oil-water interface (M = 0.016 mm^3, SD = 0.0029 mm^3) is significantly
278 greater than the control group with access to an air-water interface (M = 0.007 mm^3, SD = 0.001
279 mm^3) (One-way ANOVA with Tukey post-test, $p < 0.0001$). Furthermore, oil-exposed wild types
280 have statistically similar swim bladder volumes to that of *lhfpl5b* mutants (M = 0.014 mm^3, SD =
281 0.0038 mm^3) (One-way ANOVA with Tukey post-test, $p = 0.886$) (Figure 5C). Lateral line mutants
282 overfill their swim bladders to statistically similar proportions when presented with either an air-
283 water or oil-water interface (M = 0.01 mm^3, SD = 0.0026 mm^3) (One-way ANOVA with Tukey
284 post-test, p = 0.133). We conclude that surface tension is one of the surface characteristics the
285 lateral line is capable of detecting during initial swim bladder inflation.

286 *Optogenetic activation of lateral line hair cells prevents hyperinflation in lateral line mutant larvae*

287 If hydrodynamic information is informing the surfacing behaviors of larval fish, then
288 stimulus-independent manipulations of lateral line activity should alter their ability to correctly
289 inflate their swim bladders. To test this, we created the *Tg(lhfpl5b2028:ChR2-EYFP-PA)*
290 transgenic line that expresses the blue light activated channel, Channelrhodopsin-2, specifically in
291 lateral line hair cells (See Methods, Supplemental Figure 4). We predicted that optogenetic
292 stimulation of *lhfpl5b* mutants, whose lateral lines are insensitive to physical stimuli, would reduce
293 the frequency of the hyperinflation phenotype. Consistent with these predictions, under blue-light
294 stimulation, lateral line mutants with the *lhfpl5b:ChR2* transgene do not exhibit positive buoyancy
295 and have a significant decrease in average swim bladder volume (M = 0.0046 mm^3, SD = 0.0034
296 mm^3) compared to unstimulated transgenic mutants (M = 0.012 mm^3, SD = 0.0031 mm^3) (One-
297 way ANOVA with Tukey post-test, p = 0.00127) (Figure 6B). Transgenic wild types under blue
298 light exhibit a non-significant decrease in swim bladder volume (M = 0.0052 mm^3, SD = 0.004
299 mm^3) compared to unstimulated transgenic siblings (M = 0.0079 mm^3, SD = 0.002 mm^3) (One-way
300 ANOVA with Tukey post-test, p = 0.458). To demonstrate that blue light stimulation is reducing
301 swim bladder volumes via activation of lateral line hair cells, we treated wild type *lhfpl5b:ChR2*
302 larvae with CuSO4. As expected, we observe hyperinflation following CuSO4 treatment in
303 stimulated wild type *lhfpl5b:ChR2* larvae, with an average swim bladder volume (WT: M = 0.012
304 mm^3, SD = 0.0037 mm^3) that is statistically similar to experimental non-transgenic *lhfpl5b* mutants
305 (M = 0.011 mm^3, SD = 0.0024 mm^3) (One-way ANOVA with Tukey post-test, p = 0.998)
306 (Supplemental Figure 4B). Overall, optogenetic activation of mechanically-insensitive lateral line

organs in *lhfpl5b* mutants prevents the hyperinflation phenotype. Together, these data support the hypothesis that the lateral line provides crucial sensory information during initial swim bladder inflation in larval zebrafish.

Lateral line mutants exhibit abnormal surfacing behaviors

Our results suggest that larval fish are using their head neuromasts to sense the interfacial tension between air and water at the surface. Even in wild type zebrafish, the interaction with the surface during initial swim bladder inflation is not well characterized. To study this behavior in more detail, we quantified the number of unique visits to the surface and the amount of time per visit spent within the meniscus region from videos of wild type (n = 7) and mutant (n = 14) larvae at 4 dpf. *lhfpl5b* mutants that will over-inflate their swim bladders make more visits (M = 87.3, SD = 17.4) to the surface compared to both wild type (M = 42.0, SD = 16.3) and mutant siblings that will inflate to normal proportions (M = 31.9, SD = 19.2) (One-way ANOVA with Tukey post-test, p = 0.0004) (Figure 7A). Mutants destined for hyperinflation also spend more time (M = 139.0 s, SD = 31.6 s) at the surface than normally-inflated wild type (M = 51.9 s, SD = 24.7 s) and mutant siblings (M = 42.3 s, SD = 29.5 s) (One-way ANOVA with Tukey post-test, p = 0.00006) (Figure 7B). Since excess surfacing could be due to some mutants initiating the behavior earlier, we also documented the time of the first surfacing event and found no significant difference between neutrally buoyant and over-inflated larvae (Figure 7C). We conclude there is a correlation between how larvae interact with the surface during the initial swim bladder inflation period and their resulting swim bladder volume and buoyancy status.

Discussion

The intake of exogenous air from the surface is a common feature for intitial swim bladder inflation in many species of fish [40–44]. However, few studies have considered what sensory information is required to achieve neutral buoyancy. In this study, we describe a new role for the mechanosensory lateral line in mediating initial inflation of the swim bladder in zebrafish (Figure 8). Our data support a model in which larval zebrafish use their head neuromasts to detect the air-water interface in support of their transition to neutral buoyancy.

Lateral line defects in lhfpl5b mutants are responsible for hyperinflation phenotypes

lhfpl5b mutant zebrafish are the first genetic model for the specific loss of lateral line function in any organism [30]. These “lateral line mutants” exhibit an uncommon swim bladder

337 hyperinflation phenotype that prompted us to investigate this novel connection between lateral line
338 sensation and initial inflation of the swim bladder (Figure 1). Previous studies have demonstrated
339 that restricting access to surface air during the initial inflation period prevents swim bladder
340 inflation in larval zebrafish [40,45]. In addition, one study showed that some *solute carrier family*
341 *12 member 2* (*slc12a2 / nkcc1)* mutant zebrafish over-fill their swim bladders and that blocking
342 access to the surface prevents this phenotype [32], though further studies are required to determine
343 the cause of over-inflation in *slc12a2* mutants. Likewise, we find that blocking access to the air-
344 water interface eliminates over-inflation in lateral line mutants and greatly decreases average swim
345 bladder volumes of both mutant and wild type larvae (Figure 2). Our method of blocking access to
346 the air-water interface resulted in a small proportion of larvae (both wild type and mutant) inflating
347 their swim bladder to normal proportions, though hyperinflation was never observed. Inflation was
348 likely achieved by larvae accessing air bubbles that remain in the water after submerging the filter
349 [40]. Overall, the hyperinflation phenotype in lateral line mutants requires an intake of exogenous
350 air, pointing to a sensory defect in *lhfpl5b* mutants rather than a physiological one.

351 In support of this sensory-deficit hypothesis, we show the hyperinflation phenotype is
352 prevented by either transgenic rescue of *lhfpl5* function specifically in hair cells or optogenetic
353 stimulation of mechanically-insensitive lateral line hair cells in *lhfpl5b* mutants (Figures 3 and 6).
354 Furthermore, chemical ablation of lateral line hair cells in wild type larvae prior to initial inflation
355 can phenocopy the *lhfpl5b* mutant. A single treatment with CuSO4 caused similar swim bladder
356 over-inflation proportions to lateral line mutants (Supplemental Figure 2). Repeated neomycin
357 treatments over 3-4 dpf caused the next highest percentage of swim bladder over-inflation and a
358 single neomycin treatment only resulted in a few cases of wild type over-inflation. These results
359 agree with previous work showing rapid hair cell regeneration following neomycin treatment and
360 comparatively slower recovery after CuSO4 exposure [36,46–49]. Thus, via multiple genetic and
361 chemical approaches, our data show that lateral line hair cell activity can modulate swim bladder
362 inflation in larval zebrafish.

363 Ototoxins have been extensively used to study lateral line-mediated behaviors in free-
364 swimming larvae and adult fish [19,20,50–52]. However, we are not aware of any behavioral
365 studies where the lateral line was disrupted prior to larvae achieving neutral buoyancy, likely
366 explaining why this connection between the lateral line and initial swim bladder inflation has not
367 been noted in current literature. Interestingly, an 1896 study predicted a relationship between the

368 lateral line and swim bladder inflation, since disruption of the lateral line in adult goldfish resulted
369 in "swelling of the swim bladder" and positive buoyancy [53]. However, it is not clear if the
370 phenotypic similarities between these adult goldfish and our experimental larval zebrafish share
371 the same underlying causes. Regarding roles for the lateral line in early life behaviors, a close
372 parallel to our findings is the report that unhatched red-eyed treefrogs use their lateral line organ to
373 mediate mechanosensory-cued hatching [54]. In this case, the frog lateral line can sense vibrational
374 stimuli, such as that produced by predators, and promote escape hatching behaviors even before
375 the onset of vestibular function. Similarly, our data suggest that the lateral line is modulating early
376 locomotor activities in zebrafish prior to the development of fully formed vestibular or rheotactic
377 responses [55–57]. As such, the involvement of lateral line in the surfacing behavior may represent
378 the earliest behavioral role for the lateral line yet described.

379 *Head neuromasts are required for normal swim bladder inflation, likely by sensing surface tension*

380 We expanded on the full-body lateral line ablation experiments with specific ablations of
381 either the head or truck neuromasts with CuSO4. Previous studies have shown that head neuromasts
382 are involved with detection of surface features and prey capture [21,58–60]. Indeed, ablation of the
383 head neuromasts in wild type larvae recapitulated the hyperinflation phenotype of *lhfpl5b* mutants
384 while ablation of the tail neuromasts had no effect on either swim bladder volume or buoyancy
385 (Figure 4). These findings suggest that the head neuromasts interact with the air-water interface
386 during surfacing and that the posterior lateral line is dispensible for achieving neutral buoyancy.
387 As such, our findings also provide additional support for the anterior lateral line as a central
388 mediator of surface-related behaviors in fish.

389 The interfacial tension between air and water represents a unique hydrodynamic stimulus
390 that may be detected by the lateral line. The tension between oil and water is half that of air and
391 water [37]. Thus, by adding a layer of oil to the surface, we predicted that surface detection would
392 become increasingly difficult and result in over-filling of the swim bladder. We find that, when
393 given access to an oil-water interface, wild type larvae over-fill their swim bladders with oil to a
394 statistically similar volume as lateral line mutants who overinflate with air (Figure 6). We interpret
395 this result as support for the hypothesis that the lateral line senses interfacial tension between air
396 and water as larvae interact with the surface during initial swim bladder inflation. This
397 interpretation is further supported by the observation that *lhfpl5b* mutants (who are already
398 insensitive to interfacial tension) exhibit similar swim bladder volumes when exposed to either oil

399 or air. However, a possible complementary interpretation for these data is that larvae who fill their
400 swim bladders with oil may be deprived of the normal feedback on buoyancy levels as they intake
401 from the surface. Since oil is denser than air, oil-filled larvae are negatively buoyant. In this
402 scenario, larvae may continue to visit the surface for air intake in an attempt to achieve neutral
403 buoyancy. However, future studies are required to examine if such a feedback mechanism exists in
404 larval zebrafish.

405 *Swim bladder over-inflation is correlated with excess time spent at the air-water interface*

406 Since our data suggest that the air-water interface is providing a distinct stimulus to the
407 lateral line, we investigated whether surface interactions differed between hyperinflated *lhfpl5b*
408 mutants and their wild type counterparts. As predicted, over-inflated mutants took more visits *and*
409 spent more time at the surface than neutrally-buoyant mutant and wild type siblings (Figure 7).
410 Excess breaching of the surface occurred despite over-inflated and neutrally buoyant larvae
411 exhibiting similar timing for their first surfacing attempts. While it is unclear whether larvae ingest
412 air during the entirety of the duration spent above the air-water interface, it is known that surface
413 breaches are observed during initial inflation [2,11,40]. Therefore, the increase in surface visits
414 likely leads to an increase in air deposition to the swim bladder in lateral line mutants.

415 *Multisensory integration during the surfacing behavior*

416 Interestingly, approximately half of all lateral line mutants inflate their swim bladders to
417 normal proportions and continue to develop into viable adults. To account for this fact, we
418 hypothesize that additional somatosensory, photosensory, or mechanosensory systems may
419 compensate for the loss of lateral line sensation and help mutant larvae achieve neutral buoyancy
420 [15,16,61]. The lateral line is involved several multi-sensory behaviors, including flow orientation
421 [62–64], prey capture [21,65,66], and predator avoidance [23,54,67], and we predict that surfacing
422 can be added to this list.

423 The photosensory and mechanosensory systems exhibit distinct organizational patterns for
424 primary input to the central nervous system — even the anterior and posterior lateral line ganglia
425 primary projections are somatotopically organized in zebrafish larvae [68–73]. The Mauthner
426 neurons integrate multisensory input at the level of the hindbrain, but the surfacing behavior is
427 unlikely to use this circuit. For higher order processing however, information from the lateral line,
428 vestibular, and photosensory systems are integrated in various brain regions. The thalamus is one
429 such sensory integration center in zebrafish [74]. Socially-relevant mechanosensory and

430 photosensory information is represented in a thalamic region marked by the expression of
431 *parathyroid hormone 2* (*pth2*) and *somatostatin 7* (*sst7*) [24,26,75]. Vestibular information is also
432 represented in the thalamus [76,77], though it is not clear if the exact same region is involved.
433 Photosensory, lateral line, and vestibular/auditory information is also integrated in the tectum [76–
434 79]. In fact, neurons in the periventricular layer (PVL) of the tectum, which is similar to the superior
435 colliculus in mammals, respond to visual, auditory, and lateral line inputs [80–83]. However, it is
436 hypothesized that most of these modalities are processed in parallel at younger stages of
437 development [83]. It is worth noting that these sensory systems are in developing stages during
438 surfacing behaviors.

439 Photosensory cues did not alter the buoyancy status of either wild type or *lhfpl5b* mutant
440 larvae (Supplemental Figure 1), suggesting that, at most, photosensory systems play a subtle
441 modulatory role in the surfacing behavior of larval zebrafish. The vestibular system is likely
442 required to coordinate the vertical orientation and climbing portions of surfacing [38,56,84].
443 Meanwhile, our data support the idea that the lateral line is responsible for the surface detection
444 and breaching aspects of surfacing. However, given that both the vestibular and lateral line systems
445 are providing spatial information in during the surfacing behavior, there may be crosstalk between
446 them. For example, the vestibular system must quickly adapt to a dynamic increase in buoyancy
447 over the course of multiple breaching events, so feedback from the lateral line during surface
448 interactions may help fine tune the vestibular sense. However, the link between these systems have
449 not been well-investigated during deliberate behaviors like surfacing [85,86]. So, while sensory
450 integration exists in zebrafish and seems necessary for larvae to achieve neutral buoyancy, the
451 integration dynamics are unclear during the intial swim bladder inflation timeframe and require
452 future investigation.

453 **Acknowledgements**

454 The authors would like to thank Dr. Fadi Issa (ECU) for his support and technical advice. The
455 authors also thank the Issa, Trapani, and Erickson lab members for fish care and maintenance.

456 **Author contributions**

457 Conceptualization: A.V., T.E.; Methodology: A.V., J.G.T., T.E.; Validation: A.V.; Formal
458 analysis: A.V.; Investigation: A.V.; Resources: S.T-B., J.G.T; Writing - original draft: A.V., T.E.;
459 Writing - review & editing: A.V., J.G.T., T.E..; Visualization: A.V.; Supervision: T.E.; Project
460 administration: T.E.; Funding acquisition: J.G.T., T.E.

Funding

This work was supported by funding from East Carolina University's Division of Research, Economic Development and Engagement (REDE) and a Natural Science and Engineering Research Council (NSERC) Discovery Grant (RGPIN-2021-03166) to T.E., a National Institute on Deafness and Other Communication Disorders (NIDCD) award to J.G.T. (NIH R15DC014843), and East Carolina Department of Biology funding provided to A.V..

References

1. Alexander RM. Physical aspects of swimbladder function. Biological reviews of the Cambridge Philosophical Society. John Wiley & Sons, Ltd; 1966. pp. 141–176. doi:10.1111/j.1469-185x.1966.tb01542.x
2. Lindsey BW, Smith FM, Croll RP. From inflation to flotation: Contribution of the swimbladder to whole-body density and swimming depth during development of the zebrafish (Danio rerio). Zebrafish. 2010;7: 85–96. doi:10.1089/zeb.2009.0616
3. Evans HM, Damant GCC. Observations on the Physiology of the Swim Bladder in Cyprinoid Fishes. Journal of Experimental Biology. 1928;6: 42–55.
4. v. Ledebur JF. Beiträge zur Physiologie der Schwimmblase der Fische. Z Vgl Physiol. 1928;8: 445–460. doi:10.1007/BF00338968
5. Tait JS. The First Filling Of The Swim Bladder In Salmonoids. Can J Zool. 1960;38: 179–187. doi:10.1139/z60-021
6. Bailey HC, Doroshov SI. The duration of the interval associated with successful inflation of the swimbladder in larval striped bass (Morone saxatilis). Aquaculture. 1995;131: 135–143. doi:10.1016/0044-8486(94)00215-A
7. Kitajima C, Watanabe T, Tsukashima Y, Fujita S. Lordotic Deformation and Abnormal Development of Swim Bladders in Some Hatchery-Bred Marine Physoclistous Fish in Japan. J World Aquac Soc. 1994;25: 64–77. doi:10.1111/j.1749-7345.1994.tb00806.x
8. Chatain B. Problems related to the lack of functional swimbladder in intensive rearing of Dicentrarchus labrax and Sparus auratus. Advances in Tropical Aquaculture, Workshop at Tahiti, French Polynesia, 20 Feb - 4 Mar 1989. 1989 [cited 16 Jan 2021]. Available: https://archimer.ifremer.fr/doc/00000/1432/
9. Kimmel CB, Ballard WW, Kimmel SR, Ullmann B, Schilling TF. Stages of embryonic development of the zebrafish. Developmental Dynamics. 1995;203: 253–310. doi:10.1002/aja.1002030302
10. Doroshev S, Cornacchia J, Hogan K. Initial swim bladder inflation in the larvae of physoclistous fishes and its importance for larval culture. Rapports et Proces-verbaux des Réunions Cons int Explor Mer. 1981;178: 495–500.
11. Rieger PW, Summerfelt RC. Microvideography of gas bladder inflation in larval walleye. J Fish Biol. 1998;53: 93–99. doi:10.1111/J.1095-8649.1998.TB00112.X
12. Fero K, Yokogawa T, Burgess HA. The behavioral repertoire of larval zebrafish. Neuromethods. 2011;52: 249–291. doi:10.1007/978-1-60761-922-2_12
13. Schoppik D, Bianco IH, Prober DA, Douglass AD, Robson DN, Li JMB, et al. Gaze-stabilizing central vestibular neurons project asymmetrically to extraocular motoneuron pools. Journal of Neuroscience. 2017;37: 11353–11365. doi:10.1523/JNEUROSCI.1711-17.2017
14. Nicolson T, Rüsch A, Friedrich RW, Granato M, Ruppersberg JP, Nüsslein-Volhard C. Genetic analysis of vertebrate sensory hair cell mechanosensation: The zebrafish circler mutants. Neuron. 1998;20: 271–283. doi:10.1016/S0896-6273(00)80455-9
15. Riley BB, Moorman SJ. Development of utricular otoliths, but not saccular otoliths, is necessary for vestibular function and survival in zebrafish. J Neurobiol. 2000;43: 329–337. doi:10.1002/1097-4695(20000615)43:4<329::AID-NEU2>3.0.CO;2-H
16. Trotter AJ, Battaglene SC, Pankhurst PM. Effects of photoperiod and light intensity on initial swim bladder inflation, growth and post-inflation viability in cultured striped

trumpeter (Latris lineata) larvae. Aquaculture. 2003;224: 141–158. doi:10.1016/S0044-8486(03)00212-6

17. Villamizar N, García-Alcazar A, Sánchez-Vázquez FJ. Effect of light spectrum and photoperiod on the growth, development and survival of European sea bass (Dicentrarchus labrax) larvae. Aquaculture. 2009;292: 80–86. doi:10.1016/j.aquaculture.2009.03.045

18. Stuart KR, Drawbridge M. The effect of photoperiod on larval culture performance of two marine finfish species. Aquaculture. 2012;360–361: 54–57. doi:10.1016/j.aquaculture.2012.07.017

19. Montgomery JC, Baker CF, Carton AG. The lateral line can mediate rheotaxis in fish. Nature. 1997;389: 960–963. doi:10.1038/40135

20. Bleckmann H. The Lateral Line System of Fish. Fish Physiology. 2006. pp. 411–453. doi:10.1016/S1546-5098(06)25010-6

21. Carrillo A, McHenry MJ. Zebrafish learn to forage in the dark. Journal of Experimental Biology. 2016;219: 582–589. doi:10.1242/jeb.128918

22. Mogdans J. Sensory ecology of the fish lateral-line system: Morphological and physiological adaptations for the perception of hydrodynamic stimuli. J Fish Biol. 2019;95: 53–72. doi:10.1111/jfb.13966

23. Stewart WJ, Cardenas GS, McHenry MJ. Zebrafish larvae evade predators by sensing water flow. J Exp Biol. 2013;216: 388–98. doi:10.1242/jeb.072751

24. Anneser L, Alcantara IC, Gemmer A, Mirkes K, Ryu S, Schuman EM. The neuropeptide Pth2 dynamically senses others via mechanosensation. Nature. 2020;588: 653–657. doi:10.1038/s41586-020-2988-z

25. Butler JM, Maruska KP. Mechanosensory signaling as a potential mode of communication during social interactions in fishes. J Exp Biol. 2016;219: 2781–2789. doi:10.1242/jeb.133801

26. Venuto A, Smith CP, Cameron-Pack M, Erickson T. Alone in a crowd: effect of a nonfunctional lateral line on expression of the social hormone parathyroid hormone 2. Biol Open. 2022;11. doi:10.1242/bio.059432

27. Bleckmann H, Schwartz E. The functional significance of frequency modulation within a wave train for prey localization in the surface-feeding fishAplocheilus lineatus (Cyprinodontidae). Journal of Comparative Physiology A. 1982;145: 331–339. doi:10.1007/BF00619337

28. Gibbs MA. Lateral Line Receptors: Where Do They Come from Developmentally and Where Is Our Research Going? Brain Behav Evol. 2004;64: 163–181. doi:10.1159/000079745

29. Tsukamoto Y, Yoshino S. A Study of the Lateral-line System in Fish II. On the Relation between the Function of the Lateral-line Organ and the Habits of Fish. Japanese Journal of Ichthyology. 1957;6: 131–135. doi:10.11369/jji1950.6.131

30. Erickson T, Pacentine IV, Venuto A, Clemens R, Nicolson T. The lhfpl5 Ohnologs lhfpl5a and lhfpl5b Are Required for Mechanotransduction in Distinct Populations of Sensory Hair Cells in Zebrafish. Front Mol Neurosci. 2020;12: 320. doi:10.3389/fnmol.2019.00320

31. McCune AR, Carlson RL. Twenty ways to lose your bladder: Common natural mutants in zebrafish and widespread convergence of swim bladder loss among teleost fishes. Evol Dev. 2004;6: 246–259. doi:10.1111/J.1525-142X.2004.04030.X

32. Abbas L, Whitfield TT. Nkcc1 (Slc12a2) is required for the regulation of endolymph volume in the otic vesicle and swim bladder volume in the zebrafish larva. Development. 2009;136: 2837–2848. doi:10.1242/DEV.034215

559 33. Westerfield M. The zebrafish book. A guide for the laboratory use of zebrafish (Danio
560 rerio). 4th ed. Eugene OR: University of Oregon; 2000. Available:
561 http://zfin.org/zf_info/zfbook/zfbk.html
562 34. Erickson T, Morgan CP, Olt J, Hardy K, Busch-Nentwich E, Maeda R, et al. Integration of
563 Tmc1/2 into the mechanotransduction complex in zebrafish hair cells is regulated by
564 Transmembrane O-methyltransferase (Tomt). Elife. 2017;6. doi:10.7554/eLife.28474
565 35. Kwan KM, Fujimoto E, Grabher C, Mangum BD, Hardy ME, Campbell DS, et al. The
566 Tol2kit: a multisite gateway-based construction kit for Tol2 transposon transgenesis
567 constructs. Dev Dyn. 2007;236: 3088–3099. doi:10.1002/DVDY.21343
568 36. Venuto A, Erickson T. Evaluating the Death and Recovery of Lateral Line Hair Cells
569 Following Repeated Neomycin Treatments. Life 2021, Vol 11, Page 1180. 2021;11: 1180.
570 doi:10.3390/LIFE11111180
571 37. Johansen EM. The Interfacial Tension between Petroleum Products and Water. Ind Eng
572 Chem. 1924;16: 132–135.
573 38. Ehrlich DE, Schoppik D. Control of Movement Initiation Underlies the Development of
574 Balance. Current Biology. 2017;27: 334–344. doi:10.1016/j.cub.2016.12.003
575 39. R Core Team. R: A Language and Environment for Statistical Computing. Vienna,
576 Austria; 2022. Available: https://www.r-project.org/
577 40. Goolish EM, Okutake K. Lack of gas bladder inflation by the larvae of zebrafish in the
578 absence of an air-water interface. J Fish Biol. 1999;55: 1054–1063. doi:10.1111/j.1095-
579 8649.1999.tb00740.x
580 41. v. Ledebur JF, Wunder W. Beiträge zur Physiologie der Schwimmblase der Fische.
581 Zeitschrift für vergleichende Physiologie 1937 25:2. 1937;25: 149–155.
582 doi:10.1007/BF00339307
583 42. Jones FRH, Marshall NB. The structure and functions of the teleostean swimbladder.
584 Biological Reviews. 1953;28: 16–82. doi:10.1111/j.1469-185X.1953.tb01370.x
585 43. Furukawa S, Machida Y, Takeuchi K, Hoshikawa Y, Irie K. Failure to gulp surface air
586 induces swim bladder adenomas in Japanese medaka (Oryzias latipes). J Toxicol Pathol.
587 2022;35: 237–246. doi:10.1293/TOX.2022-0030
588 44. Korsøen ØJ, Fosseidengen JE, Kristiansen TS, Oppedal F, Bui S, Dempster T. Atlantic
589 salmon (Salmo salar L.) in a submerged sea-cage adapt rapidly to re-fill their swim
590 bladders in an underwater air filled dome. Aquac Eng. 2012;51: 1–6.
591 doi:10.1016/J.AQUAENG.2012.04.001
592 45. Lindsey BW, Dumbarton TC, Moorman SJ, Smith FM, Croll RP. Effects of simulated
593 microgravity on the development of the swimbladder and buoyancy control in larval
594 zebrafish (Danio rerio). J Exp Zool A Ecol Genet Physiol. 2011;315A: 302–313.
595 doi:10.1002/jez.677
596 46. Murakami SL, Cunningham LL, Werner LA, Bauer E, Pujol R, Raible DW, et al.
597 Developmental differences in susceptibility to neomycin-induced hair cell death in the
598 lateral line neuromasts of zebrafish (Danio rerio). Hear Res. 2003;186: 47–56.
599 doi:10.1016/S0378-5955(03)00259-4
600 47. Santos F, MacDonald G, Rubel EW, Raible DW. Lateral line hair cell maturation is a
601 determinant of aminoglycoside susceptibility in zebrafish (Danio rerio). Hear Res.
602 2006;213: 25–33. doi:10.1016/j.heares.2005.12.009
603 48. Hernández PP, Moreno V, Olivari FA, Allende ML. Sub-lethal concentrations of
604 waterborne copper are toxic to lateral line neuromasts in zebrafish (Danio rerio). Hear Res.
605 2006;213: 1–10. doi:10.1016/j.heares.2005.10.015

606 49. Mackenzie SM, Raible DW. Proliferative Regeneration of Zebrafish Lateral Line Hair
607 Cells after Different Ototoxic Insults. PLoS One. 2012;7: 47257.
608 doi:10.1371/JOURNAL.PONE.0047257
609 50. Baker CF, Montgomery JC. The sensory basis of rheotaxis in the blind Mexican cave fish,
610 Astyanax fasciatus. J Comp Physiol A. 1999;184: 519–527. doi:10.1007/s003590050351
611 51. Pavlov DS, Tyuryukov SN. The role of lateral-line organs and equilibrium in the behavior
612 and orientation of the dace, Leuciscus leuciscus, in a turbulent flow. J Ichthyol. 1993;33:
613 45–55.
614 52. Coffin AB, Ramcharitar J. Chemical Ototoxicity of the Fish Inner Ear and Lateral Line
615 BT - Fish Hearing and Bioacoustics: An Anthology in Honor of Arthur N. Popper and
616 Richard R. Fay. In: Sisneros JA, editor. Cham: Springer International Publishing; 2016.
617 pp. 419–437. doi:10.1007/978-3-319-21059-9_18
618 53. Richard MJ. Comptes rendus des séances de la Société de biologie et de ses filiales.
619 Paris,Masson [etc.]; 1896. Available: https://www.biodiversitylibrary.org/item/100656
620 54. Jung J, Serrano-Rojas SJ, Warkentin KM. Multimodal mechanosensing enables treefrog
621 embryos to escape egg-predators. J Exp Biol. 2020;223. doi:10.1242/jeb.236141
622 55. Mo W, Chen F, Nechiporuk A, Nicolson T. Quantification of vestibular-induced eye
623 movements in zebrafish larvae. BMC Neurosci. 2010;11: 110. doi:10.1186/1471-2202-11-
624 110
625 56. Bagnall MW, Schoppik D. Development of vestibular behaviors in zebrafish. Curr Opin
626 Neurobiol. 2018;53: 83–89. doi:10.1016/j.conb.2018.06.004
627 57. Olive R, Wolf S, Dubreuil A, Bormuth V, Debrégeas G, Candelier R. Rheotaxis of Larval
628 Zebrafish: Behavioral Study of a Multi-Sensory Process. Front Syst Neurosci. 2016;10.
629 doi:10.3389/fnsys.2016.00014
630 58. Müller U, Schwartz E. Influence of single neuromasts on prey localizing behavior of the
631 surface feeding fish, Aplocheilus lineatus. Journal of Comparative Physiology A.
632 1982;149: 399–408. doi:10.1007/BF00619155
633 59. Schwartz E, Hasler AD. Perception of Surface Waves by the Blackstripe Topminnow,
634 *Fundulus notatus*. Journal of the Fisheries Research Board of Canada. 1966;23: 1331–
635 1352. doi:10.1139/f66-124
636 60. Bleckmann H. Prey Identification and Prey Localization in Surface-feeding Fish and
637 Fishing Spiders. Sensory Biology of Aquatic Animals. New York, NY: Springer New
638 York; 1988. pp. 619–641. doi:10.1007/978-1-4612-3714-3_24
639 61. Suchocki CR, Sepulveda-Villet OJ. The role of phototaxis in the initial swim bladder
640 inflation of larval yellow perch (Perca flavescens). Int Aquat Res. 2019;11: 33–42.
641 doi:10.1007/s40071-019-0217-x
642 62. Liao JC. The role of the lateral line and vision on body kinematics and hydrodynamic
643 preference of rainbow trout in turbulent flow. J Exp Biol. 2006;209: 4077–90.
644 doi:10.1242/jeb.02487
645 63. Bak-Coleman J, Court A, Paley DA, Coombs S. The spatiotemporal dynamics of
646 rheotactic behavior depends on flow speed and available sensory information. J Exp Biol.
647 2013;216: 4011–24. doi:10.1242/jeb.090480
648 64. Coombs S, Bak-Coleman J, Montgomery J. Rheotaxis revisited: a multi-behavioral and
649 multisensory perspective on how fish orient to flow. Journal of Experimental Biology.
650 2020;223. doi:10.1242/JEB.223008
651 65. New JG. Multimodal Integration in the Feeding Behaviors of Predatory Teleost Fishes.
652 Brain Behav Evol. 2002;59: 177–189. doi:10.1159/000064905

653 66. Nelson ME, MacIver MA, Coombs S. Modeling Electrosensory and Mechanosensory
654 Images during the Predatory Behavior of Weakly Electric Fish. Brain Behav Evol.
655 2002;59: 199–210. doi:10.1159/000064907
656 67. Free BA, McHenry MJ, Paley DA. Probabilistic analytical modelling of predator–prey
657 interactions in fishes. J R Soc Interface. 2019;16: 20180873. doi:10.1098/rsif.2018.0873
658 68. McCormick CA. Central Lateral Line Mechanosensory Pathways in Bony Fish. The
659 Mechanosensory Lateral Line. 1989; 341–364. doi:10.1007/978-1-4612-3560-6_17
660 69. Mirjany M, Faber DS. Characteristics of the anterior lateral line nerve input to the
661 Mauthner cell. Journal of Experimental Biology. 2011;214: 3368–3377.
662 doi:10.1242/JEB.056226
663 70. Hale ME, Katz HR, Peek MY, Fremont RT. Neural circuits that drive startle behavior,
664 with a focus on the Mauthner cells and spiral fiber neurons of fishes. https://doi-
665 org.proxy.hil.unb.ca/101080/0167706320161182526. 2016;30: 89–100.
666 doi:10.1080/01677063.2016.1182526
667 71. Alexandre D, Ghysen A, Ghysen A. Somatotopy of the lateral line projection in larval
668 zebrafish. Proc Natl Acad Sci U S A. 1999;96: 7558–62. doi:10.1073/pnas.96.13.7558
669 72. Liao JC, Haehnel M. Physiology of afferent neurons in larval zebrafish provides a
670 functional framework for lateral line somatotopy. J Neurophysiol. 2012;107: 2615–2623.
671 doi:10.1152/jn.01108.2011
672 73. Fame RM, Brajon C, Ghysen A. Second-order projection from the posterior lateral line in
673 the early zebrafish brain. Neural Dev. 2006;1: 4. doi:10.1186/1749-8104-1-4
674 74. Mueller T. What is the thalamus in zebrafish? Frontiers in Neuroscience. Frontiers; 2012.
675 p. 64. doi:10.3389/fnins.2012.00064
676 75. Kappel JM, Förster D, Slangewal K, Shainer I, Svara F, Donovan JC, et al. Visual
677 recognition of social signals by a tectothalamic neural circuit. Nature 2022 608:7921.
678 2022;608: 146–152. doi:10.1038/s41586-022-04925-5
679 76. Migault G, Plas TL van der, Trentesaux H, Panier T, Candelier R, Proville R, et al. Whole-
680 Brain Calcium Imaging during Physiological Vestibular Stimulation in Larval Zebrafish.
681 Current Biology. 2018;28: 3723-3735.e6. doi:10.1016/J.CUB.2018.10.017
682 77. Favre-Bulle IA, Vanwalleghem G, Taylor MA, Rubinsztein-Dunlop H, Scott EK. Cellular-
683 Resolution Imaging of Vestibular Processing across the Larval Zebrafish Brain. Current
684 Biology. 2018;28: 3711-3722.e3. doi:10.1016/j.cub.2018.09.060
685 78. Isa T, Marquez-Legorreta E, Grillner S, Scott EK. The tectum/superior colliculus as the
686 vertebrate solution for spatial sensory integration and action. Current Biology. 2021;31:
687 R741–R762. doi:10.1016/j.cub.2021.04.001
688 79. Filosa A, Barker AJ, Dal Maschio M, Baier H. Feeding State Modulates Behavioral
689 Choice and Processing of Prey Stimuli in the Zebrafish Tectum. Neuron. 2016;90: 596–
690 608. doi:10.1016/J.NEURON.2016.03.014
691 80. Perrault TJ, Stein BE, Rowland BA. Non-stationarity in multisensory neurons in the
692 superior colliculus. Front Psychol. 2011;2. doi:10.3389/FPSYG.2011.00144
693 81. King AJ, Schnupp JWH, Carlile S, Smith AL, Thompson ID. The development of
694 topographically-aligned maps of visual and auditory space in the superior colliculus. Prog
695 Brain Res. 1996;112: 335–350. doi:10.1016/S0079-6123(08)63340-3
696 82. Ingle D. Evolutionary perspectives on the function of the optic tectum. Brain Behav Evol.
697 1973;8: 211–237. doi:10.1159/000124355

698 83. Thompson AW, Vanwalleghem GC, Heap LA, Scott EK. Functional profiles of visual-,
699 auditory-, and water flow-responsive neurons in the Zebrafish Tectum. Current Biology.
700 2016;26: 743–754. doi:10.1016/j.cub.2016.01.041
701 84. Ehrlich DE, Schoppik D. A primal role for the vestibular sense in the development of
702 coordinated locomotion. Elife. 2019;8. doi:10.7554/eLife.45839
703 85. Liu Z, Hildebrand DGC, Morgan JL, Slimmon N, Bagnall MW. The organization of the
704 gravity-sensing system in zebrafish. bioRxiv. 2021; 2021.07.09.451839.
705 doi:10.1101/2021.07.09.451839
706 86. Chagnaud BP, Engelmann J, Fritzsch B, Glover JC, Straka H. Sensing External and Self-
707 Motion with Hair Cells: A Comparison of the Lateral Line and Vestibular Systems from a
708 Developmental and Evolutionary Perspective. Brain Behav Evol. 2017;90: 98–116.
709 doi:10.1159/000456646
710
711

712 **Figures**

713

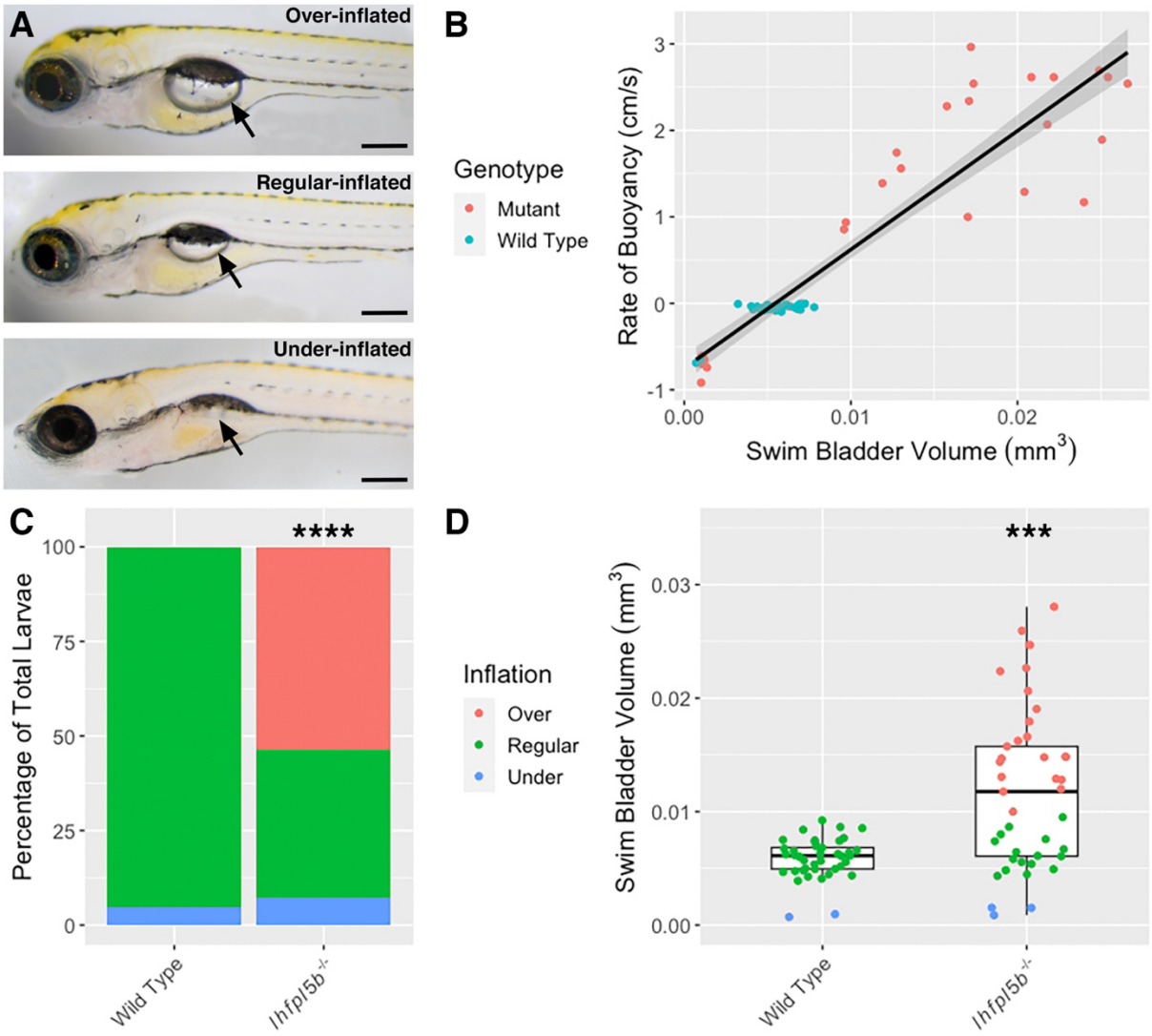

714

715 **Figure 1**. Hyperinflation of the swim bladder in lateral line mutants (*lhfpl5b*$^{-/-}$). A) Representative
716 examples of over-, regular, and under-inflated swim bladders (arrows) in larval zebrafish at 6 dpf
717 (top: *lhfpl5b*$^{-/-}$, others are wild type). B) Correlation between buoyancy and swim bladder volume.
718 Line of best fit applied through the combination of mutant and wild type data (linear model, R-
719 squared = 0.8574). C) Percentage of larvae that exhibit over-, regular, and under-inflation of the
720 swim bladder, as defined by positive, neutral, and negative buoyancy. A Chi-Squared Test was
721 used to determine significance. D) Swim bladder volume (mm^3) in wild type and *lhfpl5b* mutant
722 larvae at 6 dpf. A Welch's t-test was used to determine significance. *** = $p < 0.001$, **** = $p <$
723 0.0001. Scale bar = 0.2 mm.

724

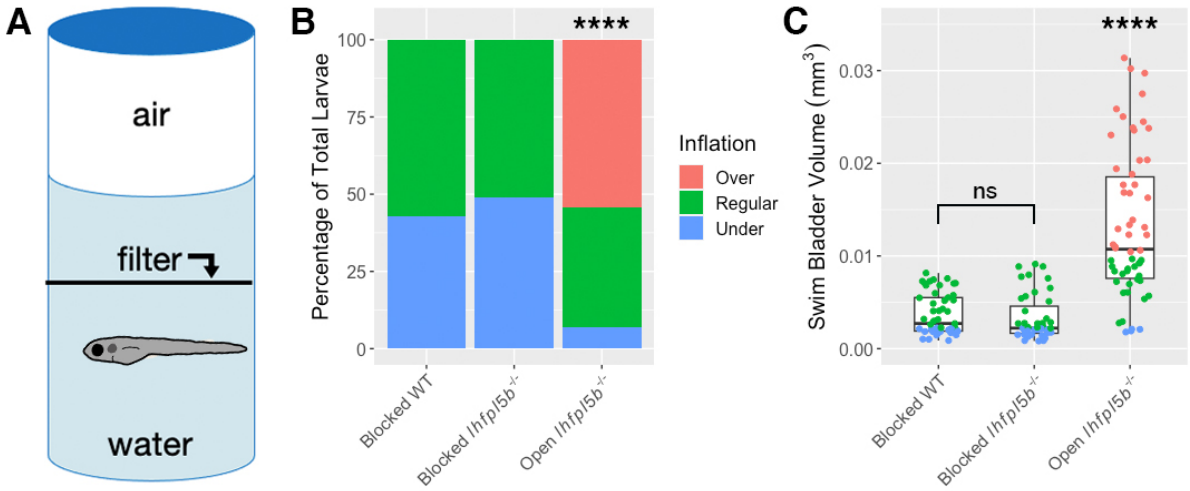

Figure 2: Blocking access to the surface eliminates the hyperinflation phenotype in lateral line mutants (*lhfpl5b*$^{-/-}$). A) Diagram of experimental set up with a filter blocking access to the surface. B) Percentage of larvae that exhibit over-, regular, and under-inflation of the swim bladder at 6 dpf. A Chi-Squared Test was used to determine significance. C) Swim bladder volume (mm^3) of larvae at 6 dpf. A One-Way ANOVA was used to determine significance. **** = $p < 0.0001$, , **** = $p < 0.0001$, ns = no significance. Full ANOVA table in supplemental tables.

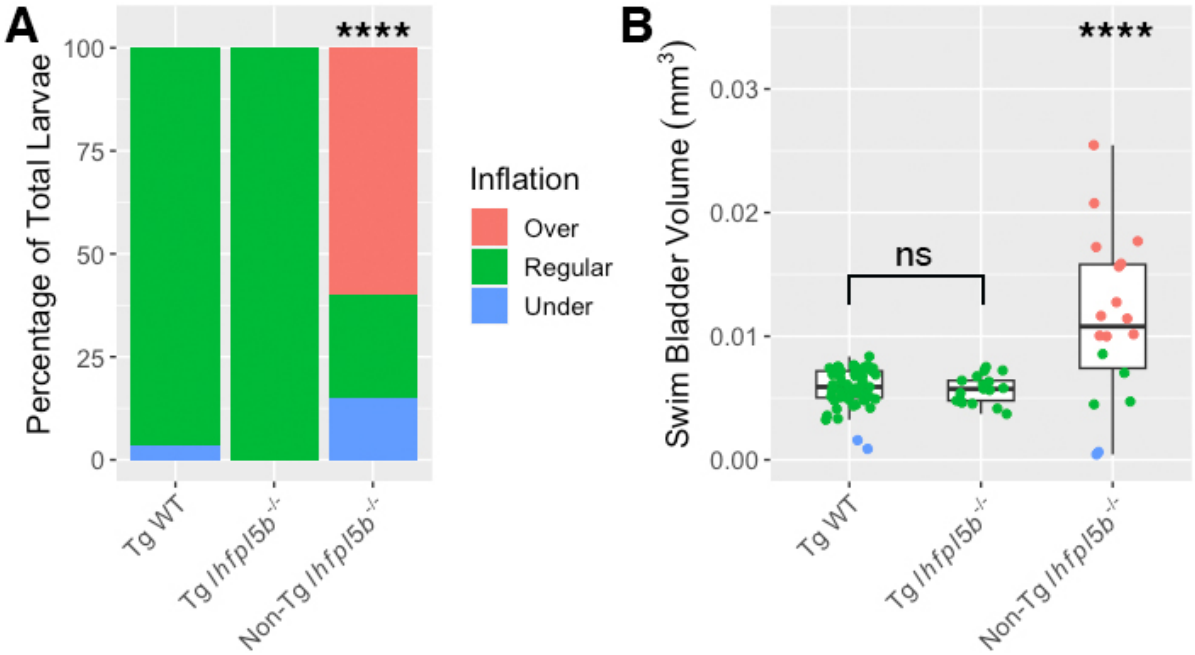

Figure 3: Rescue of lateral line mutants (*lhfpl5b*$^{-/-}$) with the *Tg(myo6b:EGFP-lhfpl5a)vo23* transgene. A) Percentage of larvae that exhibit swim bladder under, regular, and over-inflation at 6 dpf. A Chi-Squared Test was used to determine significance. B) Swim bladder volume (mm^3) of larvae at 6 dpf. A One-Way ANOVA was used to determine significance. **** = $p < 0.0001$, ns = no significance. Full ANOVA table in supplemental tables.

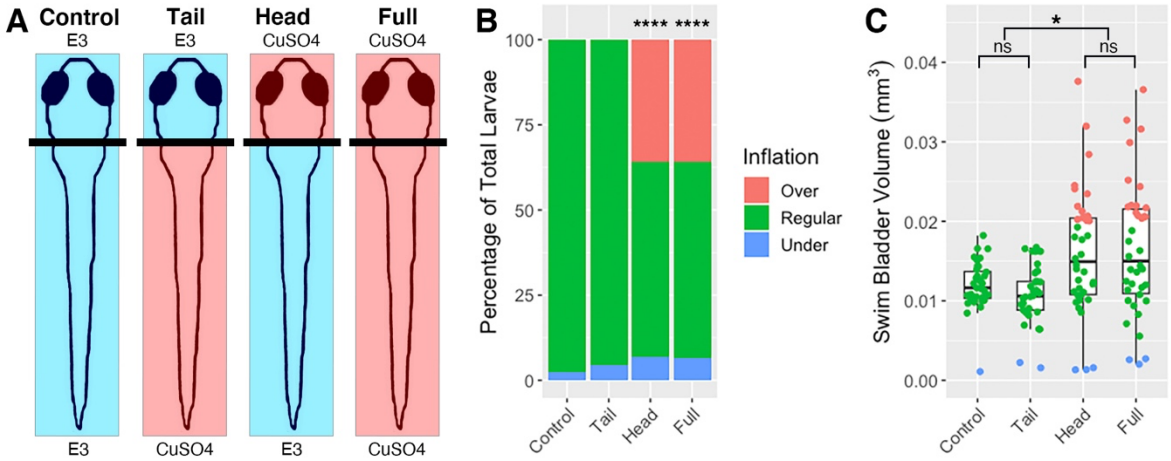

Figure 4: Head-specific ablations of the lateral line recapitulates the *lhfpl5b* mutant hyperinflation phenotype. A) Diagram of experiment. B) Percentage of larvae that exhibit swim bladder under, regular, and over-inflation at 5 dpf. A Chi-Squared Test was used to determine significance. C) Swim bladder volume (mm^3) of larvae at 5 dpf. A One-Way ANOVA was used to determine significance. * = $p < 0.05$, , **** = $p < 0.0001$, ns = no significance. Full ANOVA table in supplemental tables. Images of live larvae following treatment in Supplemental Figure 3.

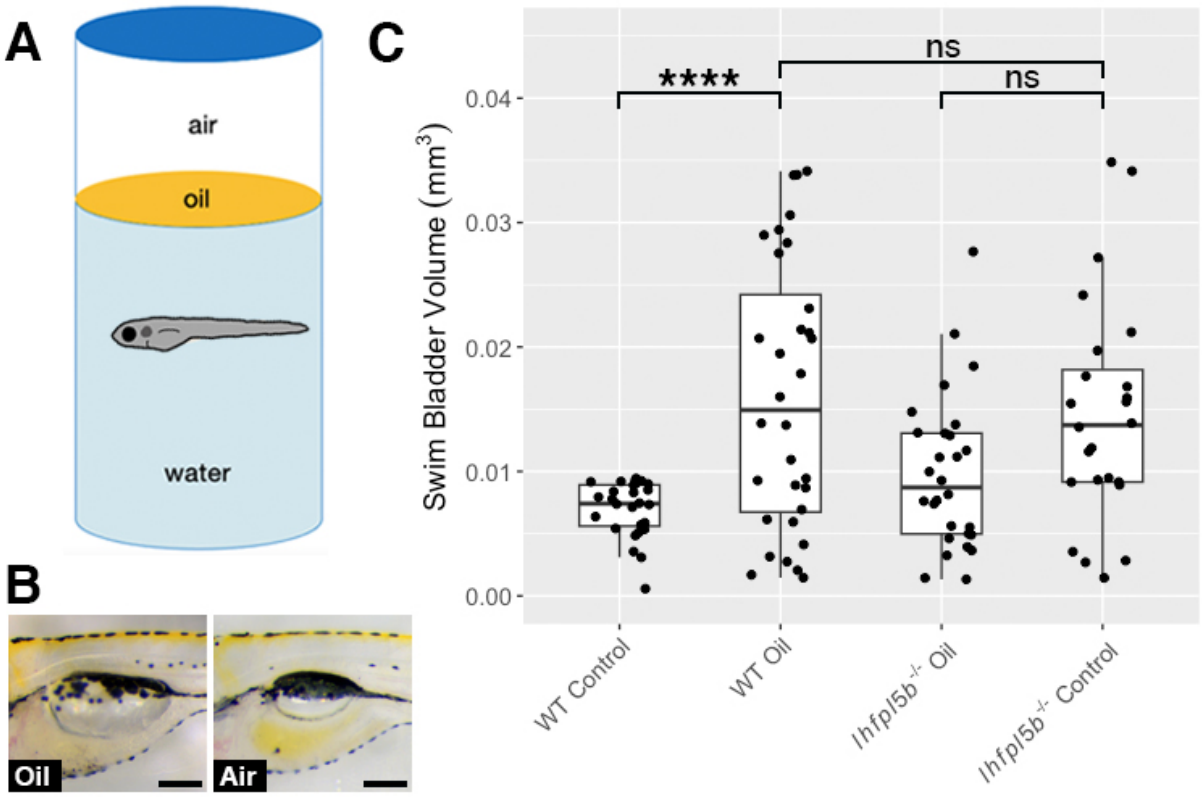

Figure 5: Decreasing interfacial surface tension with mineral oil results in over-filling of the swim bladder. A) Diagram of experiment with 2 mm layer of oil on surface. B) Images of swim bladder phenotypes resulting from surface oil and surface air exposure in wild type larvae at 6 dpf. C) Swim bladder volume (mm^3) at 6 dpf. A One-Way ANOVA was used to determine significance. * = $p < 0.05$, ns = no significance. Scale bar = 0.1 mm. Full ANOVA table in supplemental tables.

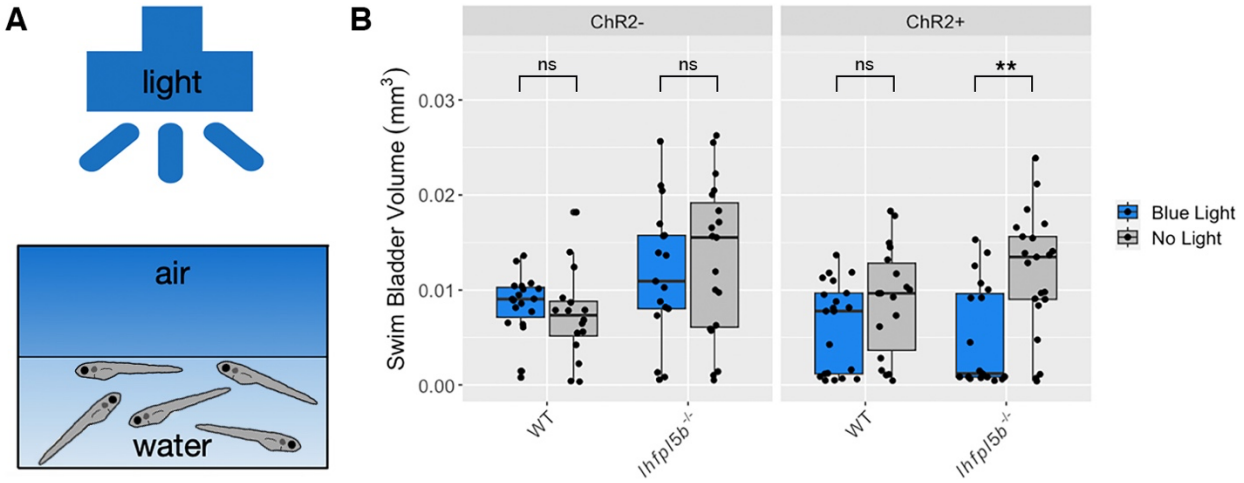

Figure 6: Optogenetic activation of lateral line hair cells with Channelrhodopsin-2 (ChR2) in wild type and *lhfpl5b* mutant larval zebrafish. A) Diagram of experiment with blue light overhead flashing for 25 ms with 1 s intervals. Treatments were started at 4 dpf and swim bladder volume was assessed at 6 dpf. B) Swim bladder volume (mm^3) of larvae at 6 dpf, n = 16-21 per condition. One-Way ANOVA was used to determine significance. ** = $p < 0.001$, ns = no significance. Full ANOVA table in supplemental tables.

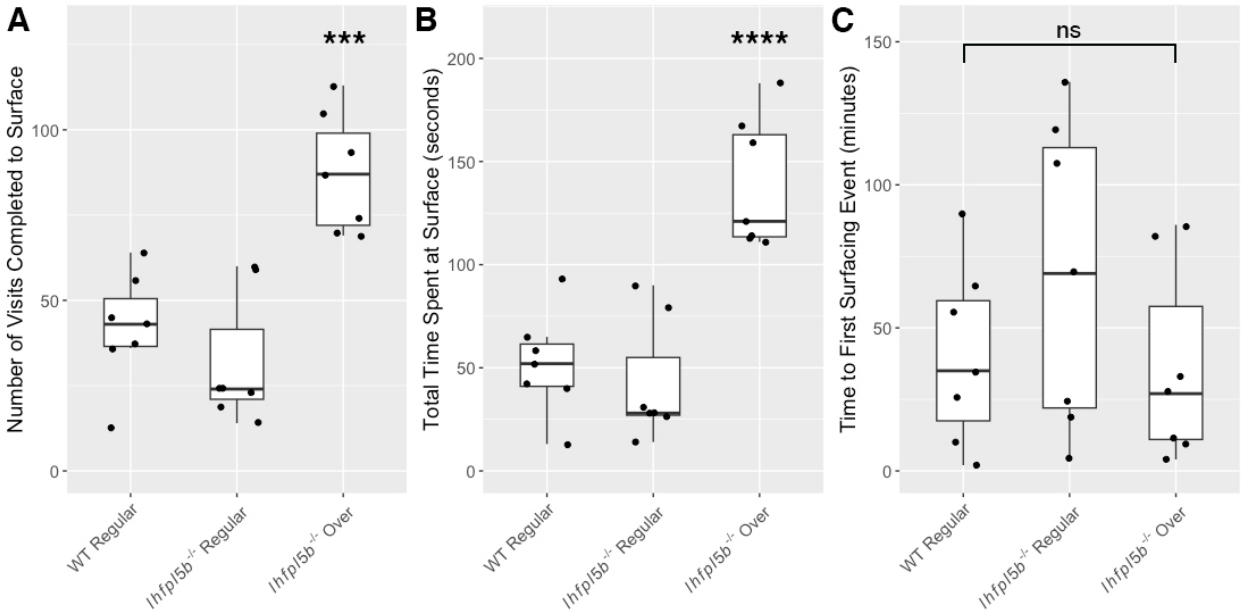

Figure 7: Quantification of the surfacing behaviors of wild type and *lhfpl5b* mutant zebrafish larvae during initial swim bladder inflation. A) Total number of individual visits taken by larval fish to the air-water interface on 4 dpf for 12 hours (9 AM – 9 PM). B) Total amount of time larval fish spend at the surface for all visits combined on 4 dpf. C) Time to first surface visit after access was allowed. A One-Way ANOVA was used to determine significance. *** = $p < 0.001$, ns = no significance.

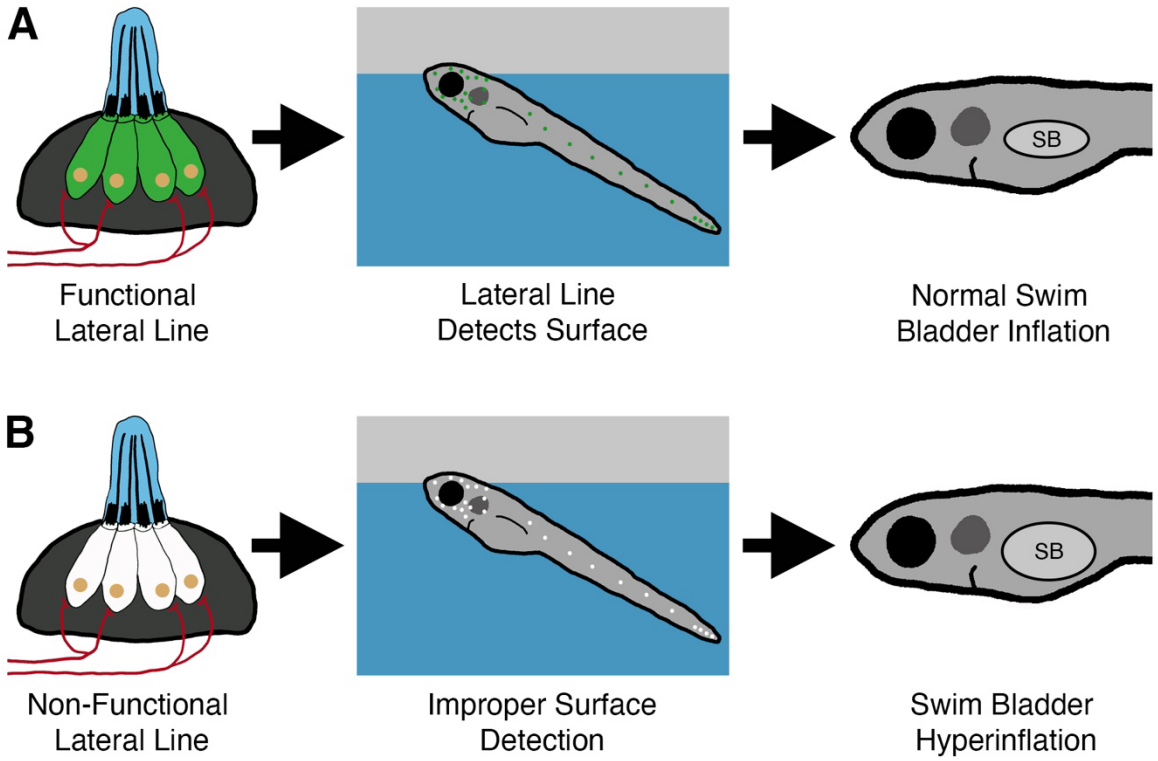

Figure 8. Summary of the surfacing behavior of wild type and lateral line-deficient zebrafish larvae. A) Wild type larvae use their lateral line hair cells (in green) to mediate interactions with the air-water interface during surfacing. As a result of accurate surface detection, larvae take in an appropriate volume of air for swim bladder (SB) inflation and achieve neutral buoyancy. B) Larvae with a genetic loss of lateral line function (hair cells in white) misinterpret the air-water interface, leading to increased interactions with the surface. Consequently, lateral line mutants *(lhfpl5b*$^{-/-}$*)* take in an excess volume of air, resulting in hyperinflation of the swim bladder for approximately half of mutant larvae. Selective chemical ablations of the head neuromasts produce similar results, implicating the anterior lateral line as the primary sensory organ for interactions with the air-water interface during the surfacing behavior.

783 **Supplemental Figures**

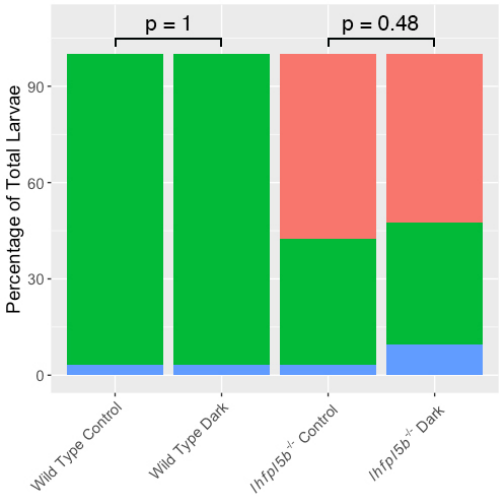

784
785 **Supplemental Figure 1.** Buoyancy status of larvae raised in total darkness. Percentage of larvae
786 that exhibit swim bladder under, regular, and over-inflation raised in either a 14:10 light/dark
787 cycle (Control) or total darkness (0:24 light/dark cycle). A Chi-Squared Test was used to assess
788 significance. Both Wild Type Control and Wild Type Dark over-inflation proportions: M = 0.0%,
789 SD = 0.0%, n = 32. *lhfpl5b*$^{-/-}$ Control over-inflation proportion: M = 57.5%, SD = 6.6%, n = 30.
790 *lhfpl5b*$^{-/-}$ Dark over-inflation proportion: M = 52.4%, SD = 4.1%, n = 30.
791

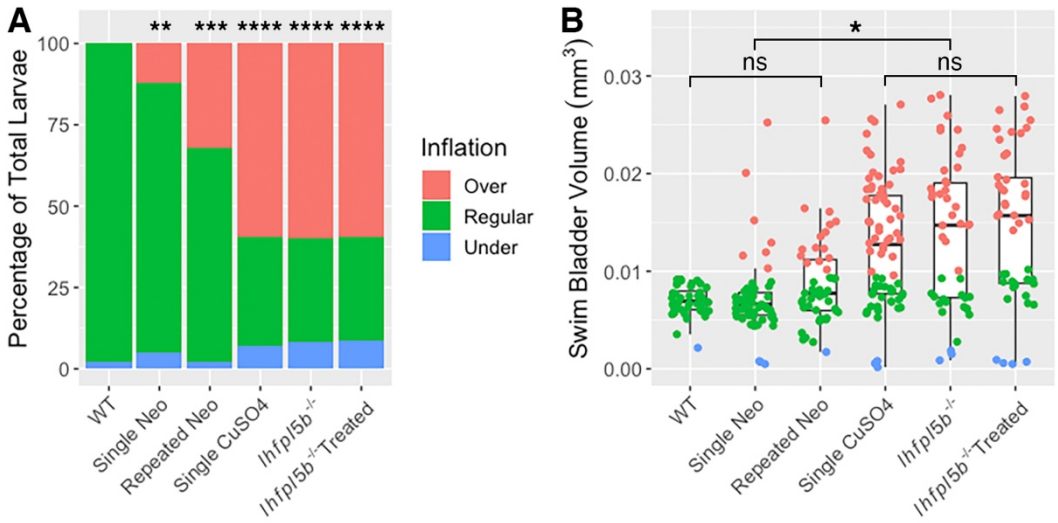

Supplemental Figure 2. Chemical ablations of lateral line hair cells phenocopies the hyperinflation phenotype of *lhfpl5b* mutants. A) Percentage of larvae treated with either neomycin or CuSO4 that exhibit swim bladder under, regular, and over-inflation. A Chi-Squared Test was used to assess significance. B) Swim bladder volume (mm^3) in 5 dpf larvae treated with either neomycin or CuSO4. A One-Way ANOVA was used to determine significance. **** = $p < 0.0001$, *** = $p < 0.001$, ** = $p < 0.01$, * = $p < 0.05$, ns = no significance. A full ANOVA table can be found in the supplemental tables.

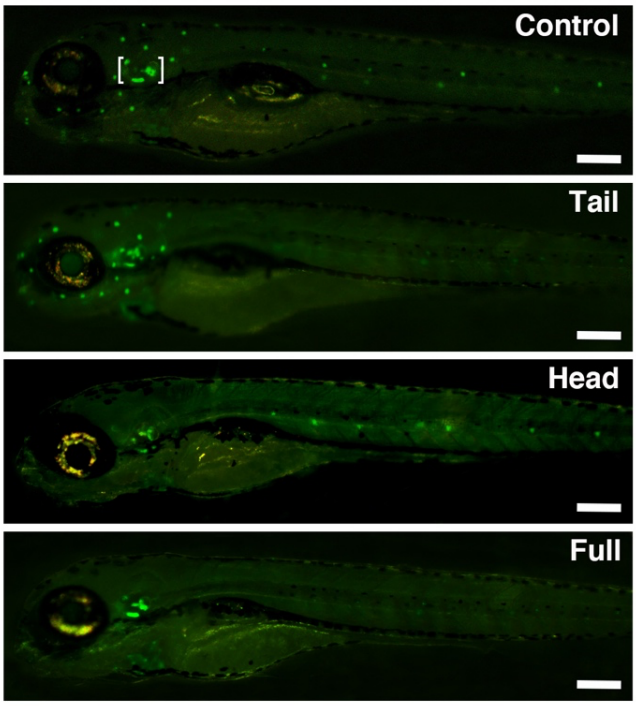

Supplemental Figure 3. Head and trunk-specific lateral line ablations with CuSO4. Representative images of live *Tg(myo6b:EGFP-PA)vo68* transgenics at 4 dpf, two hours after CuSO4 treatment. This transgene labels hair cells of the lateral line and inner ear (indicated by white brackets on the Control image). CuSO4 treatment ablates lateral line hair cells only, leaving inner ear hair cells intact.

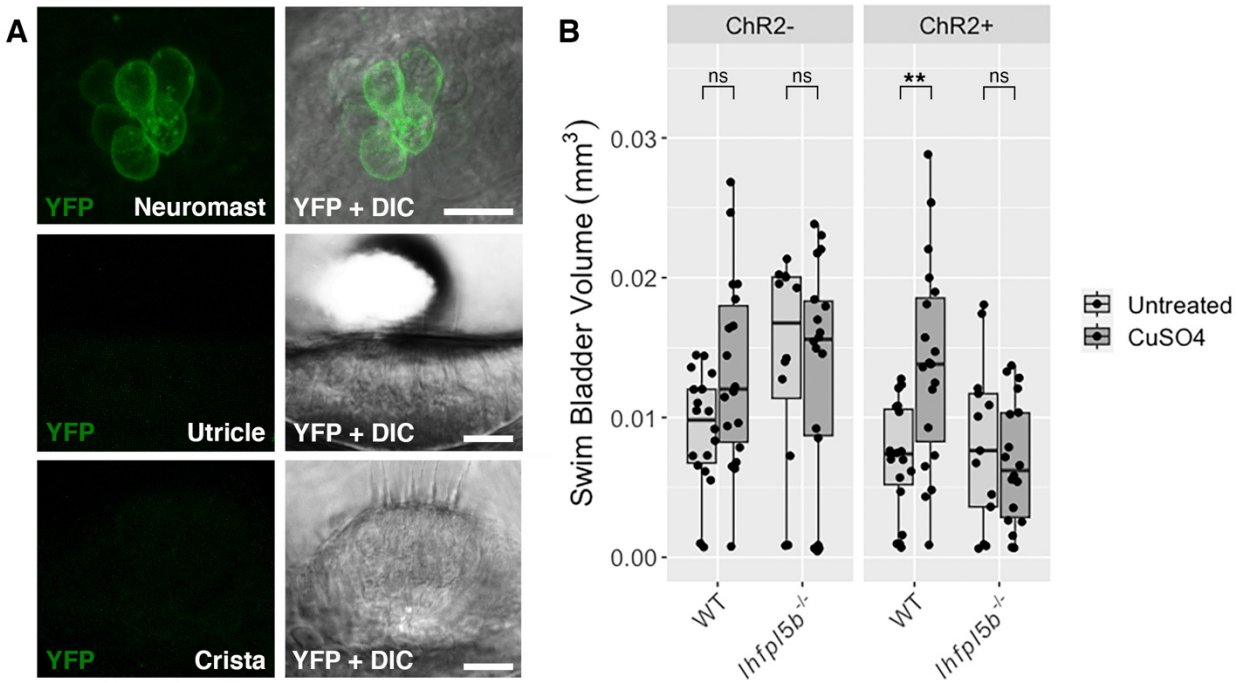

Supplemental Figure 4: A) Representative images of Channelrhodopsin-2 (ChR2) expression in neuromast, utricle, and crista hair cells of *Tg(lhfpl5b2028:ChR2-EYFP-PA)* transgenics at 2 dpf. ChR2-YFP expression is detectable only in the lateral line neuromasts, indicating specificity of the *lhfpl5b* regulatory region used to drive ChR2 expression. First panel is YFP only (false-colored green) and the second panel is a merge of YFP and DIC. Scale bars = 10 uM. B) Swim bladder volume (mm^3) of 6 dpf wild type and *lhfpl5b*$^{-/-}$ larvae, with and without the *ChR2* transgene. Groups of larvae were also treated with CuSO4 to ablate lateral line hair cells. All larvae were stimulated with blue light. The impacts of blue light stimulation on wild type ChR2 transgenics is abolished by chemical ablation of lateral line hair cells. As expected, *lhfpl5b* mutants are unaffected by CuSO4 treatment. A One-Way ANOVA was used to determine significance. ** = $p < 0.00724$, ns = no significance. A full ANOVA table can be found in the supplemental tables.